Organic & Biomolecular Chemistry

PAPER

Cite this: *Org. Biomol. Chem.*, 2017, **15**, 5635

Enzymatic conjugation using branched linkers for constructing homogeneous antibody–drug conjugates with high potency†

Yasuaki Anami,[a] Wei Xiong,[a] Xun Gui,[a] Mi Deng,[b] Cheng Cheng Zhang,[b] Ningyan Zhang,[a] Zhiqiang An[a] and Kyoji Tsuchikama *[a]

Received 27th April 2017,
Accepted 15th June 2017

DOI: 10.1039/c7ob01027c

rsc.li/obc

Antibody–drug conjugates (ADCs) are emerging therapeutic agents in the treatment of cancer, and various conjugation strategies and chemical linkers have been developed to efficiently construct ADCs. Despite previous extensive efforts for improving conjugation efficiency and ADC homogeneity, most ADC linkers developed to date load only single payloads. Branched linkers that can load multiple payload molecules have yet to be fully explored. It is logical to envisage that a multi-loading strategy allows for increase in drug-to-antibody ratio (DAR) with less chemical or enzymatic modification to the antibody structure compared to traditional linear linkers, leading to efficient ADC construction, minimal destabilization of the antibody structure, and enhanced ADC efficacy. Herein, we report that the branched linkers we designed can be quantitatively installed on an anti-HER2 monoclonal antibody by microbial transglutaminase (MTGase)-mediated conjugation without impairing its antigen binding affinity, enabling modular installation of payload molecules and construction of homogeneous ADCs with increased DARs (up to 8). An anti-HER2 antibody–monomethyl auristatin F conjugate constructed using our branched linkers showed greater *in vitro* cytotoxicity against HER2-expressing breast cancer cell lines than that consisting of linear linkers, demonstrating the effectiveness of the branched linker-based payload delivery. Our finding demonstrates that enzymatic ADC construction using branched linkers is a promising strategy, which may lead to innovative cancer therapeutics.

Introduction

Chemotherapy is one of the major clinical options in treatment of cancer, especially leukemia.[1] Although extensive studies have led to improved chemotherapeutic regimens, severe side effects derived from off-target cytotoxicity of chemotherapeutic agents often result in the deterioration of a patient's quality of life and discontinuation of treatment. Antibody–drug conjugates (ADCs), therapeutic monoclonal antibodies tethered to highly cytotoxic molecules (payloads) through chemical linkers, have emerged as a promising therapeutic format that can circumvent such issues in cancer chemotherapy.[2–4] This molecular platform enables the selective delivery of cytotoxic payloads to target cancer cells through antibody–antigen interaction and following internalization, resulting in a broader therapeutic window compared to the use of chemotherapeutic agents alone.[5] Long circulation life, preferable biodistribution and pharmacokinetic (PK) profiles of ADCs are also advantageous features from a drug development perspective. Indeed, two ADCs have been approved by the Food and Drug Administration (FDA): Adcetris®, for the treatment of CD30-positive relapsed or refractory Hodgkin's lymphoma and systemic anaplastic large cell lymphoma;[6,7] and Kadcyla®, for the treatment of human epidermal growth factor receptor 2 (HER2)-positive breast cancer.[8,9] In addition, more than 60 ADCs are in clinical trials as of 2016.[4,10]

Conjugation methods and chemical linkers are crucial factors determining the PK and stability profiles of ADCs.[11] Traditional conjugation methods are lysine–amide coupling and cysteine–maleimide coupling, which are employed for preparing the FDA-approved Adcetris® and Kadcyla®.[12,13] While simple and most frequently used, these methods yield ADCs that differ in conjugation sites and drug-to-antibody ratios (DARs). Such heterogeneous ADCs often suffer from increased clearance rates[14,15] and require strictly controlled production

[a]*Texas Therapeutics Institute, The Brown Foundation Institute of Molecular Medicine, The University of Texas Health Science Center at Houston, 1881 East Road, Houston, TX 77054, USA. E-mail: Kyoji.Tsuchikama@uth.tmc.edu*
[b]*Departments of Physiology and Developmental Biology, The University of Texas Southwestern Medical Center, 6001 Forest Park Road, Dallas, TX 75390, USA*

†Electronic supplementary information (ESI) available: Synthetic protocols, characterization of new compounds, additional figures, biological assay protocols, and assay data. See DOI: 10.1039/c7ob01027c

to minimize DAR variation.[16] To overcome this problem, site-specific conjugations have emerged as a means to construct homogeneous ADCs. Junutula and co-workers reported the THIOMAB technology that utilizes two cysteine residues incorporated by genetic engineering for linker conjugation to give ADCs with defined DARs.[17] ADCs obtained by this method showed improved PK profiles and *in vivo* efficacy compared to heterogeneous ADCs prepared by the traditional cysteine–maleimide coupling. Since then, other methods for constructing homogeneous ADCs including cysteine rebridging,[18–21] incorporation of non-natural amino acids,[22–25] and (chemo) enzymatic approaches[26–30] have been developed. Schibli and co-workers reported an antibody–linker conjugation method using a microbial transglutaminase (MTGase). Through MTGase-mediated transpeptidation, this method covalently tethers ADC linkers containing terminal primary amines to the side chain of glutamine 295 (Q295) of the human IgG heavy chain (Fig. 1).[31] In addition to use for ADC construction, this method has been utilized for the modification of other classes of proteins with various organic compounds, including DNA.[32–36]

Despite extensive efforts for improving conjugation efficiency and ADC homogeneity, most ADC linkers developed to date load only single payloads. Branched linkers that can load multiple payload molecules have yet to be fully explored. A multi-loading strategy allows for the increase in DAR with less chemical or enzymatic modification to the antibody structure compared to traditional linkers. This increase in DAR could lead to efficient ADC construction, minimal destabilization of the antibody structure, and enhanced ADC efficacy. To our knowledge, there have previously been only a handful of examples of ADCs equipped with dual-loading linkers.[37–39] A cysteine conjugation-based dual-loading linker enabling modular payload installation was recently developed.[40] Herein, we demonstrate that branched cleavable ADC linkers can be efficiently installed on a therapeutic monoclonal antibody by MTGase-mediated conjugation. This new strategy enables modular installation of payload molecules and construction of homogeneous ADCs with an increased DAR (Fig. 1). Upon antigen recognition and internalization to target cancer cells, the cathepsin B-responsive peptide sequences incorporated in our branched linkers undergo lysosomal cleavage to liberate two cytotoxic payloads per linker, leading to effective cell killing.

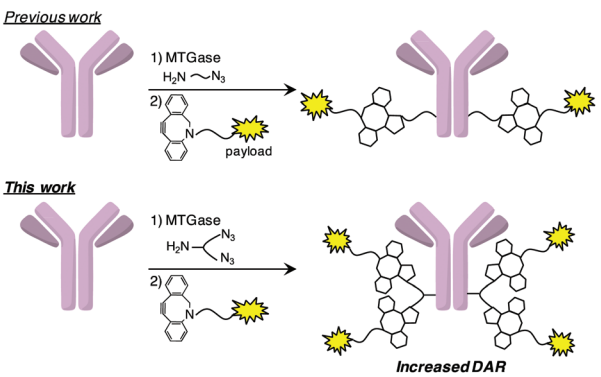

Fig. 1 MTGase-mediated antibody–drug conjugation using linear or branched linkers. Azide-containing linkers are conjugated to the side chain of Q295 of the IgG heavy chain using MTGase, followed by installation of the payload by a strain-promoted azide–alkyne cyclization to afford an ADC with a DAR of 2 (linear linker) or 4 (branched linker). MTGase, microbial transglutaminase.

Results and discussion

Assessment of cathepsin B-mediated cleavage of the branched linkers

To identify the rational design of branched ADC linkers that can release two payloads inside the target cancer cell, we synthesized a series of linear and branched fluorescent probes **1–4** (Fig. 2 and Schemes S1–S4, see ESI† for synthesis details). These model linker units consisted of cathepsin B-cleavable valine–citrulline (Val–Cit) with or without polyethyleneglycol (PEG) spacers. This dipeptide sequence has been used in many successful ADCs including the FDA-approved ADC Adcetris®.[13] The sequence is stable in circulation but in lysosomes it undergoes cathepsin B-mediated cleavage, resulting in the intracellular release of payload.[41] We also installed tryptophan and 2,4-dinitrophenylethylenediamine (EdDnp) as a fluorophore/quencher(s) pair, which is commonly used in the Förster resonance energy transfer (FRET) assay. We assessed the release of EdDnp from each synthetic model linker unit in the presence of human cathepsin B (Fig. 2 and S1†). We found that the linear PEG (+) probe **2** released EdDnp more efficiently than linear PEG (–) **1**. Gratifyingly, the release rate of the branched PEG (+) probe **4** was comparable to that of the linear PEG (+) probe **2**. In contrast, the branched PEG (–) probe **3** showed marginal release of EdDnp. We surmise that the structural congestion of the branched probe **3** due to the lack of PEG spacers prevents cathepsin B from accessing Val-Cit moieties. These results clearly illustrate that the spacer is a crucial component for retaining the high responsiveness of the Val–Cit containing linkers to cathepsin B-mediated cleavage, especially in the branched linker format.

Synthesis and conjugation of the branched linkers

With the rational linker design in hand, we set out to construct ADCs containing branched linkers. First, we designed and synthesized branched linkers **5–7** (Fig. 3). These linkers contained (1) a lysine scaffold as a branching point, (2) PEG spacers, (3) a primary amine for MTGase-mediated antibody-linker conjugation, and (4) two azide groups as reaction handles for the following payload installation by the azide–alkyne click reaction[42] (*vide infra*). We constructed these linkers by sequential amide couplings of each component (Scheme S5†). The azide and primary amine were spatially sequestered with PEG spacers to minimize the steric congestion of the linker arms. In addition, we envisaged that highly hydrophilic PEG spacers could help reduce the hydrophobicity of the ADCs to be con-

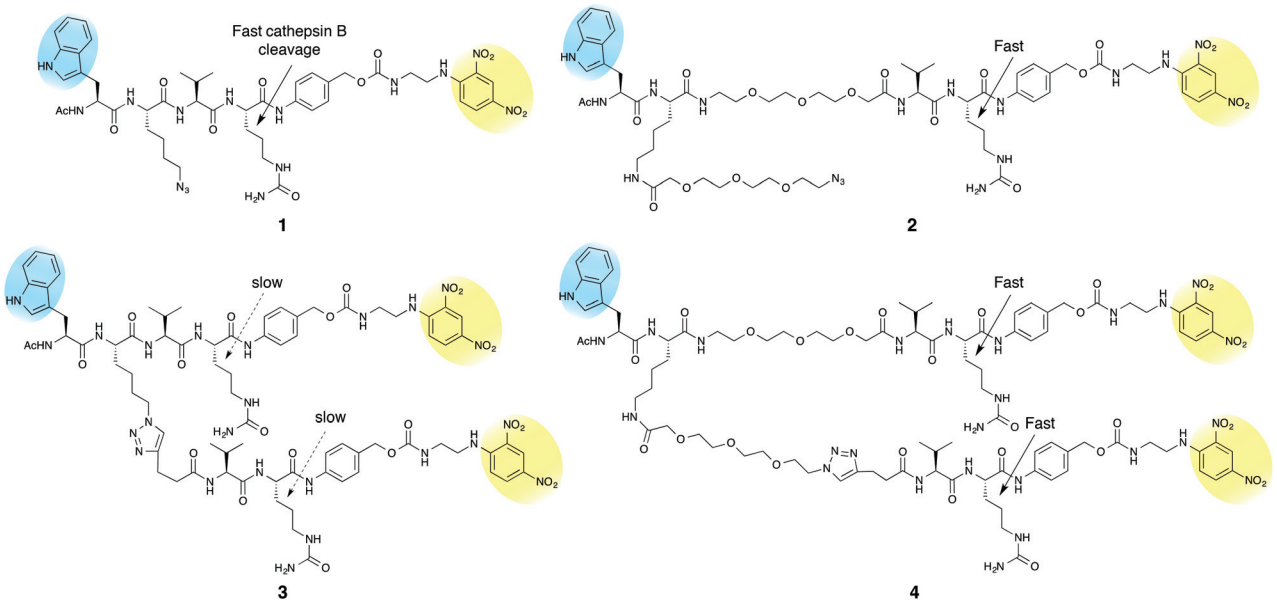

Fig. 2 Structures of fluorescent probes **1–4** containing tryptophan (fluorophore) and EdDnp groups (quencher) for the FRET assay (see the ESI† for synthesis and assay detail). The Val–Cit sequences within probes **1**, **2**, and **4** underwent cathepsin B-mediated cleavage to release the EdDnp from the probes whereas the cleavage of probe **3** was marginal.

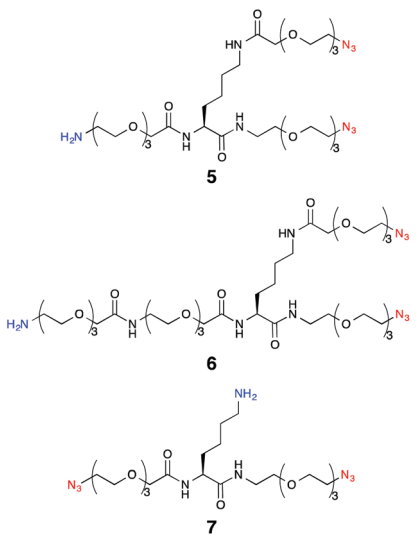

Fig. 3 Structures of branched linkers **5–7**.

structed, which is crucial to prevent protein aggregation.[43] Indeed, PEG chains installed on the payload terminus or the linker reportedly prevent ADCs forming non-covalent oligomers.[38,44]

Next, we performed a conjugation of the branched linkers synthesized to an anti-HER2 IgG1. In this study, we used an engineered anti-HER2 monoclonal antibody (mAb) with a mutation of the asparagine 297 of the heavy chain into alanine (N297A), which was developed by our group.[45] We have reported that this mutation does not alter the HER2 binding profile of the anti-HER2 mAb.[45] This mutation allowed us to omit the removal of the *N*-glycan chain on the asparagine 297, a required step for MTGase-mediated antibody-linker conjugation.[31] We attempted to install branched linkers **5–7** onto the N297A anti-HER2 mAb according to the reported protocol (linker: 80 equiv., antibody: 1.0 mg mL^{-1}, MTGase: 6.7 unit per mg^{-1} antibody).[31] However, the conversion rates were unsatisfactory (50–79%, entries 1–3 in Table 1 and Fig. S2 and S3†), resulting in mixtures of somewhat heterogeneous antibody–linker conjugates. The bulkiness of primary amine-containing molecules often leads to low efficiency in MTGase-mediated protein labeling.[46] Indeed, Schibli and co-workers used a simple linear linker for ADC construction to achieve quantitative conversion.[31] This finding made us recognize that the reaction conditions needed to be optimized to attach our bulky branched linkers to the N297A anti-HER2 mAb in an efficient manner. Thus, we screened various reaction conditions using the branched linker **5**, the most reactive linker of the three. We found that the amount of MTGase did not show a significant impact on the conversion rate (entry 4). In contrast, a higher concentration of the N297A anti-HER2 mAb substantially improved the conjugation efficiency (entry 5). In addition, increasing the amount of linker **5** turned out to be effective for improving the conversion rate (entries 6 and 7). We further examined various reaction conditions, and finally found effective conditions enabling nearly quantitative conjugation (entries 8 and 9).

Incubation of the reaction mixture at 37 °C overnight resulted in partial loss of the product probably due to protein denaturing. Thus, we decided to perform the linker conjugation in the following sections at room temperature. The

Table 1 MTGase-mediated antibody–branched linker conjugation

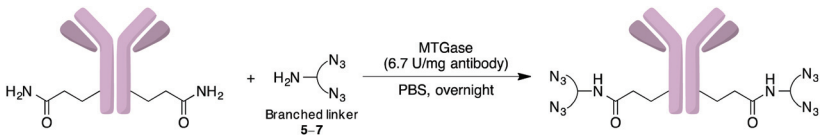

Entry	Linker (equiv.)	Linker	Antibody (mg mL^{-1})	Temperature (°C)	Conversion[b] (%)
1	80	**5**	1.0	37	79
2	80	**6**	1.0	37	52
3	80	**7**	1.0	37	50
4[a]	80	**5**	1.0	37	77
5	80	**5**	2.0	37	86
6	200	**5**	2.0	37	90
7	400	**5**	2.0	37	90
8	400	**5**	6.2	37	>95[c]
9	400	**5**	6.2	r.t.	>95
10	400	**6**	6.2	r.t.	94
11	400	**7**	6.2	r.t.	>95

[a] MTGase (26.9 U mg^{-1} antibody). [b] Determined based on deconvoluted ESI-mass spectra. [c] After 3 h. Partial loss of the product was observed after overnight incubation.

optimal reaction conditions also enabled highly efficient conjugation of branched linkers **6** and **7** to the N297A anti-HER2 mAb (entries 10 and 11). This success demonstrates that the MTGase-based transpeptidation can efficiently conjugate even bulky linkers to antibodies under optimal conditions. In addition, this finding is encouraging because additional modifications of linker structure may be adopted to fine-tune ADC physicochemical properties and further increase DARs. Our results also indicate that the MTGase-mediated transpeptidation could be used more generally for various protein modifications.

Payload installation by click chemistry and stability study

Finally, we coupled the N297A anti-HER2 mAb–branched linker **5** conjugate obtained and the potent antimitotic agent monomethyl auristatin F (MMAF), a relatively hydrophilic payload frequently used in ADCs. We employed the strain-promoted azide–alkyne cycloaddition (copper-free click reaction)[42] using the MMAF module **8** containing dibenzocyclooctyne (DBCO), PEG spacer, Val–Cit, and *p*-aminobenzyloxycarbonyl (PABC) (Fig. 4a). PABC was incorporated to allow for traceless release of MMAF upon cathepsin B-mediated cleavage of Val–Cit. The anti-HER2 mAb–linker **5** conjugate (4.0 mg mL^{-1}) was incubated with DBCO–MMAF **8** (1.5 equiv. per reaction site) in PBS/4% DMSO. The click reaction reached full completion within 1 h to give nearly homogeneous ADC **9** with an average DAR of 3.9 (determined based on UV traces, Fig. 4b, c, S4, and S5†). We also prepared two control ADCs in the same manner: an N297A anti-HER2 mAb–MMAF conjugate containing linear linkers (linear ADC **10**, DAR: 1.9)[31] and an N297A non-targeting IgG conjugated with MMAF through the branched linker **5** (non-targeting branched ADC **11**, DAR: 3.9).

The cleavable branched linkers installed on ADC **9** were stable under physiological conditions; no significant degradation of the linkers was observed in human plasma at 37 °C after 7 days, indicating that the DAR did not significantly change during incubation (Fig. S7†). Furthermore, size-exclusion chromatography (SEC) analysis revealed that ADC **9** existed predominantly in the monomer form (Fig. 4d). These results support the validity of our linker design from a drug development perspective.

It has been reported that N297Q mutated IgGs provide four conjugation sites (Q295 and Q297 per heavy chain) for the MTGase-mediated transpeptidation, enabling the installation of four linear linker–payload modules to IgGs.[27,47] Gratifyingly, we found that the branched linker **5** could be installed on a N297Q anti-HER2 mAb. Following click conjugation with MMAF module **8** yielded a high-loading ADC with an average DAR of 7.4 (Fig. S8†). Although the obtained ADC contained a small amount of lower DAR species, its homogeneity is higher than general ADCs constructed by traditional lysine or cysteine coupling. We believe that the optimization of the branched linker structure and reaction conditions for N297Q mAb-based conjugation will allow for the construction of highly homogeneous, higher DAR ADCs using our methodology. Such an effort will be reported from our laboratory in due course.

Evaluation of the ADCs for antigen binding and cytotoxicity

We evaluated anti-HER2 ADCs **9** and **10** for binding affinity and specificity to the HER2 in cell-based ELISA assays using the human breast cancer cell lines SKBR-3 (HER2 positive) and MDA-MB-231 (HER2 negative) (Fig. 5 and S9†). Branched ADC **9** showed a high binding affinity to SKBR-3, comparable to those of linear ADC **10** and the parent N297A anti-HER2 mAb (K_D = 0.98, 1.12, and 0.64 nM, respectively). In contrast, non-targeting ADC **11** did not show HER-2 specific binding. None of the ADCs bound to MDA-MB-231. These results demonstrate that the branched linker-MMAF moieties within ADC **9** do not

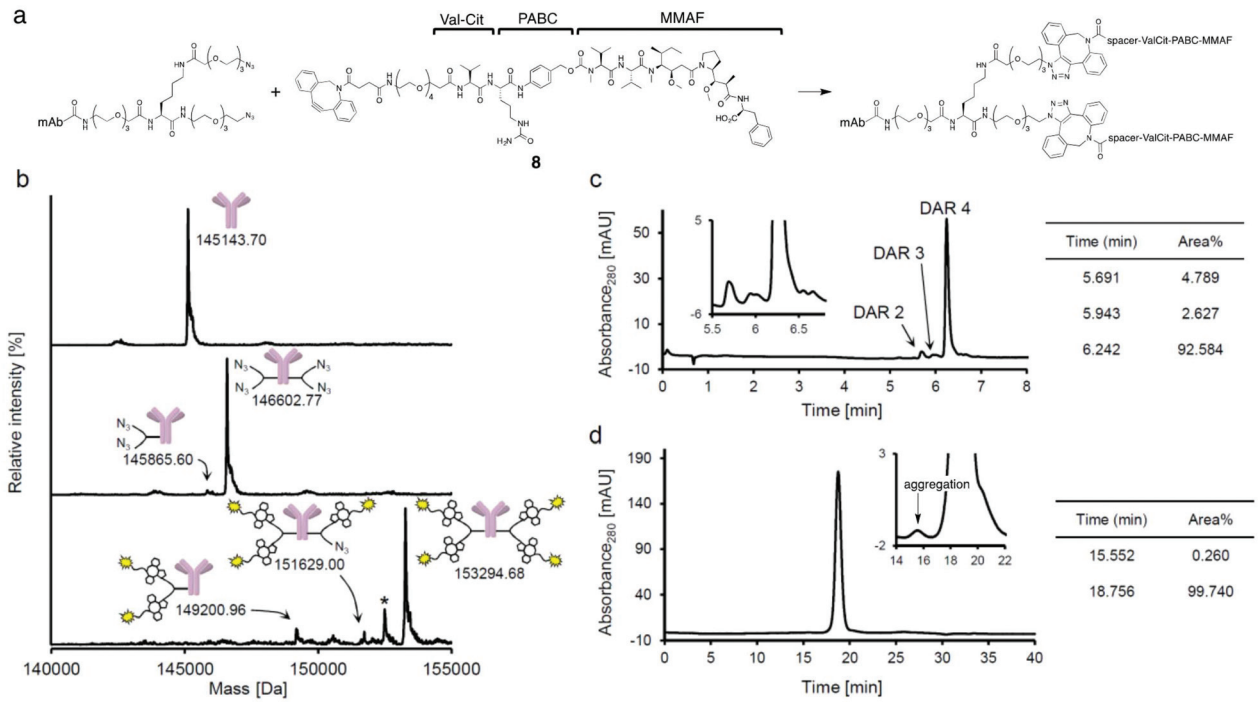

Fig. 4 Synthesis and characterization of branched ADC **9**. (a) Antibody-payload conjugation by strain-promoted azide–alkyne cyclization (copper-free click reaction). (b) Deconvoluted ESI-mass spectra. Top panel: N297A anti-HER2 mAb. Middle panel: antibody–branched linker conjugate. An antibody–linker di-conjugate was the major product and a very small amount of mono-conjugate was detected. Bottom panel: antibody–MMAF (yellow) conjugate **9**. The click reaction afforded an ADC with a DAR of 4 as the major product and small amount of ADCs with lower DARs (2 and 3). Asterisk (*) indicates a fragment ion derived from the DAR-4 product (see Fig. S6†). (c) The reverse-phase HPLC trace (UV: 280 nm) of ADC **9**. The average DAR was determined to be 3.9 based on the peak areas of each DAR species. (d) The SEC trace (UV: 280 nm) of crude ADC **9** (before purification). The small peak at 15.6 min is derived from high molecular weight proteins (protein aggregates), indicating that the monomer content of ADC **9** is >99%.

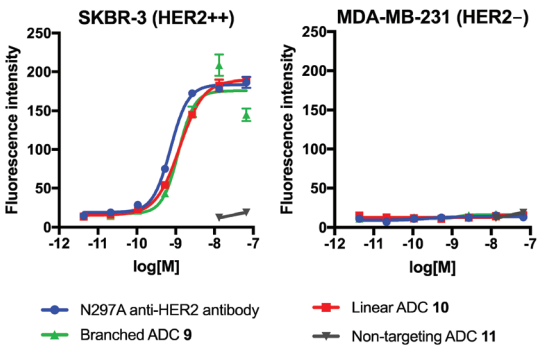

	K_D (nM)	
	SKBR-3	MDA-MB-231
N297A anti-HER2 antibody	0.64 (0.48–0.86)	–
Branched ADC **9** (DAR: 3.9)	0.98 (0.53–1.73)	–
Linear ADC **10** (DAR: 1.9)	1.12 (0.87–1.43)	–

Fig. 5 Cell-based ELISA using the SKBR-3 (HER2 positive, left) and MDA-MB-231 (HER2 negative, right) cell lines. The binding affinities of unconjugated N297A anti-HER2 mAb (blue) and ADCs **9** (green), **10** (red), and **11** (gray) against HER2 were measured. All assays were performed in triplicate. Error bars represent SEM and values in parentheses are 95% confidential intervals. All antibodies tested except **11** showed HER2-dependent cell binding.

impact the antigen recognition and specificity. As previously reported,[31] the conjugation site Q295 in the Fc moiety is distant from the antigen recognition site in the Fab region, allowing for the MTGase-based conjugation of linker–payload components at this position without detrimental effects on the antigen binding. Our results are consistent with this observation.

To investigate how the branched linker-based conjugation influences cell killing potency, we tested ADCs **9–11** and the parent N297A anti-HER2 mAb in cell-based assays using three human cell lines with varying HER2 expression levels: SKBR-3 (HER2++), MDA-MB-453 (HER2+), and MDA-MB-231 (HER2−) (Fig. 6). Branched ADC **9** (DAR: 3.9) exerted greater potency than linear ADC **10** (DAR: 1.9) in SKBR-3 (EC_{50}: 0.36 nM and 0.83 nM, respectively) whereas non-targeting ADC **11** and the unmodified N297A anti-HER2 mAb showed marginal cytotoxicity. The 2.3-fold difference between the EC_{50} values of ADCs **9** and **10** was statistically significant (confirmed by the extra sum-of-squares F test, $p < 0.0001$). In addition, the maximum cell killing effect of ADC **9** (85% cell killing at 5.3 nM) was higher than that of ADC **10** (71% cell killing at 13.3 nM) with a statistically significant difference (Student's t test, $p < 0.005$). We also observed the enhancement of ADC efficacy in the moderately HER2-positive cell line MDA-MB-453; the

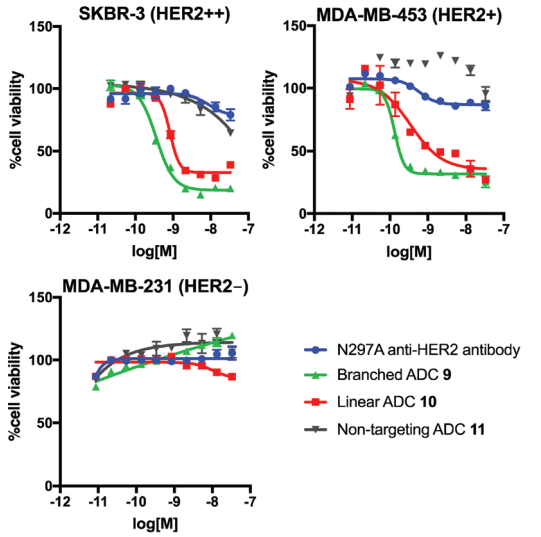

	EC_{50} (nM)		
	SKBR-3	MDA-MB-453	MDA-MB-231
Branched ADC **9** (DAR: 3.9)	0.36 ± 0.04	0.13 ± 0.01	–
Linear ADC **10** (DAR: 1.9)	0.83 ± 0.09	0.43 ± 0.26	–

Fig. 6 The *in vitro* cytotoxicity of unconjugated N297A anti-HER2 mAb (blue) and ADCs **9** (green), **10** (red), and **11** (gray). All assays were performed in triplicate. Error bars represent SEM. Branched ADC **9** showed the greatest cell killing potency both in SKBR-3 and in MDA-MB-453 of the antibodies tested. None of the antibodies tested showed significant cell killing in MDA-MB-231.

dose–response curve of branched ADC **9** clearly shifted towards lower concentrations compared to that of linear ADC **10**, resulting in EC_{50} values of 0.13 nM and 0.43 nM, respectively. Although the standard deviation of the linear ADC **10** is relatively large, we confirmed that the difference between these EC_{50} values was statistically significant ($p = 0.01$).

The observed lower EC_{50} values in MDA-MB-453 than those in highly HER2-expressing SKBR-3 may indicate that MDA-MB-453 is more sensitive to MMAF than is SKBR-3. Indeed, it has been reported that the highest level of HER2 expression does not necessarily lead to a maximal HER2-targeting ADC cell killing effect.[48] As anticipated, all ADCs tested showed no cytotoxicity to the HER2-negative MDA-MB-231. Collectively, these results clearly demonstrated that the increased DAR by our branched linker contributed to the enhancement of the ADC efficacy without impairing the cell binding and specificity of the parent antibody.

Conclusion

In this proof-of-concept study, we showed that hydrophilic branched linkers containing a primary amine and two azide groups could be efficiently installed on Q295 of an anti-HER2 mAb using MTGase under optimized conditions. The following click chemistry-based coupling of MMAF molecules afforded a nearly homogeneous ADC with a DAR of 3.9. The branched ADC constructed was found to have high stability in human plasma, high antigen binding, cell specificity, and greater *in vitro* cell killing potency than the linear ADC with a DAR of 1.9. Although we used only one mAb and one payload in this study, the MTGase-mediated branched linker conjugation presented could potentially be used for constructing various homogeneous ADCs given that the conjugation site Q295 is in the Fc region which is conserved in all human IgG isotypes and that a common antibody–branched linker conjugate prepared can be flexibly coupled with various payloads by orthogonal click chemistry reactions. Testing with various mAbs and payloads will reveal the applicability of our technology. In addition, testing of the prototype ADC constructed in this study for *in vivo* pharmacokinetics, stability, and efficacy will provide more detailed information to fine-tune the structure (*e.g.*, length of the PEG spacers) and physicochemical properties of the branched linker–payload component toward clinically relevant ADCs. Such an effort will be of crucial importance to load more hydrophobic payloads than MMAF (*e.g.*, monomethyl auristatin E and maytansinoids) as high-DAR ADCs containing hydrophobic payloads reportedly suffer from aggregation as well as rapid clearance.[43] Along with optimization of the branched linker structure, the reported methods for masking payloads using external long PEG chains may help reduce such risks.[38,44]

As a more interesting approach, installing two different reaction handles on the branched linker scaffold could enable the facile construction of ADCs loading two different payloads through click chemistry-based orthogonal couplings. Such a heterologous loading strategy will yield ADCs with dual modes of action, which is challenging to achieve with traditional linear linkers in terms of ADC homogeneity. The dual-loading ADC is an emerging format exemplified recently for combating drug-resistant tumors.[40] Altogether, the enzymatic ADC construction using branched linkers is a promising strategy for developing potent ADCs, which may lead to innovative cancer therapeutics in the future.

Conflict of interest

The authors declare no competing financial interest.

Acknowledgements

We acknowledge Dr Mohammad Y. Wani for insightful discussions and Dr Georgina T. Salazar for editing the manuscript. This work was supported by The University of Texas System (Regents Health Research Scholars Award to K. T.), the Welch Foundation (AU00024 to Z. A.), and the CPRIT (RP150551 to Z. A.).

Notes and references

1 V. T. DeVita and E. Chu, *Cancer Res.*, 2008, **68**, 8643–8653.

2 J. R. McCombs and S. C. Owen, *AAPS J.*, 2015, **17**, 339–351.
3 P. Polakis, *Pharmacol. Rev.*, 2016, **68**, 3–19.
4 K. Tsuchikama and Z. An, *Protein Cell*, 2016, DOI: 10.1007/s13238-016-0323-0.
5 R. V. J. Chari, M. L. Miller and W. C. Widdison, *Angew. Chem., Int. Ed.*, 2014, **53**, 3796–3827.
6 A. Younes, N. L. Bartlett, J. P. Leonard, D. A. Kennedy, C. M. Lynch, E. L. Sievers and A. Forero-Torres, *N. Engl. J. Med.*, 2010, **363**, 1812–1821.
7 P. D. Senter and E. L. Sievers, *Nat. Biotechnol.*, 2012, **30**, 631–637.
8 P. M. LoRusso, D. Weiss, E. Guardino, S. Girish and M. X. Sliwkowski, *Clin. Cancer Res.*, 2011, **17**, 6437–6447.
9 S. Verma, D. Miles, L. Gianni, I. E. Krop, M. Welslau, J. Baselga, M. Pegram, D.-Y. Oh, V. Dieras, E. Guardino, L. Fang, M. W. Lu, S. Olsen and K. Blackwell, *N. Engl. J. Med.*, 2012, **367**, 1783–1791.
10 N. Diamantis and U. Banerji, *Br. J. Cancer*, 2016, **114**, 362–367.
11 J. Lu, F. Jiang, A. Lu and G. Zhang, *Int. J. Mol. Sci.*, 2016, **17**, 561.
12 G. D. Lewis Phillips, G. Li, D. L. Dugger, L. M. Crocker, K. L. Parsons, E. Mai, W. A. Blättler, J. M. Lambert, R. V. J. Chari, R. J. Lutz, W. L. T. Wong, F. S. Jacobson, H. Koeppen, R. H. Schwall, S. R. Kenkare-Mitra, S. D. Spencer and M. X. Sliwkowski, *Cancer Res.*, 2008, **68**, 9280–9290.
13 J. Katz, J. E. Janik and A. Younes, *Clin. Cancer Res.*, 2011, **17**, 6428–6436.
14 K. J. Hamblett, P. D. Senter, D. F. Chace, M. M. C. Sun, J. Lenox, C. G. Cerveny, K. M. Kissler, S. X. Bernhardt, A. K. Kopcha, R. F. Zabinski, D. L. Meyer and J. A. Francisco, *Clin. Cancer Res.*, 2004, **10**, 7063–7070.
15 S. Panowski, S. Bhakta, H. Raab, P. Polakis and J. R. Junutula, *mAbs*, 2013, **6**, 34–45.
16 R. P. Lyon, D. L. Meyer, J. R. Setter and P. D. Senter, *Methods Enzymol.*, 2012, **502**, 123–138.
17 J. R. Junutula, H. Raab, S. Clark, S. Bhakta, D. D. Leipold, S. Weir, Y. Chen, M. Simpson, S. P. Tsai, M. S. Dennis, Y. Lu, Y. G. Meng, C. Ng, J. Yang, C. C. Lee, E. Duenas, J. Gorrell, V. Katta, A. Kim, K. McDorman, K. Flagella, R. Venook, S. Ross, S. D. Spencer, W. Lee Wong, H. B. Lowman, R. Vandlen, M. X. Sliwkowski, R. H. Scheller, P. Polakis and W. Mallet, *Nat. Biotechnol.*, 2008, **26**, 925–932.
18 F. Bryden, A. Maruani, H. Savoie, V. Chudasama, M. E. B. Smith, S. Caddick and R. W. Boyle, *Bioconjugate Chem.*, 2014, **25**, 611–617.
19 C. R. Behrens, E. H. Ha, L. L. Chinn, S. Bowers, G. Probst, M. Fitch-Bruhns, J. Monteon, A. Valdiosera, A. Bermudez, S. Liao-Chan, T. Wong, J. Melnick, J.-W. Theunissen, M. R. Flory, D. Houser, K. Venstrom, Z. Levashova, P. Sauer, T.-S. Migone, E. H. van der Horst, R. L. Halcomb and D. Y. Jackson, *Mol. Pharmaceutics*, 2015, **12**, 3986–3998.
20 A. Maruani, M. E. B. Smith, E. Miranda, K. A. Chester, V. Chudasama and S. Caddick, *Nat. Commun.*, 2015, **6**, 6645.
21 E. Robinson, J. P. M. Nunes, V. Vassileva, A. Maruani, J. C. F. Nogueira, M. E. B. Smith, R. B. Pedley, S. Caddick, J. R. Baker and V. Chudasama, *RSC Adv.*, 2017, **7**, 9073–9077.
22 J. Y. Axup, K. M. Bajjuri, M. Ritland, B. M. Hutchins, C. H. Kim, S. A. Kazane, R. Halder, J. S. Forsyth, A. F. Santidrian, K. Stafin, Y. Lu, H. Tran, A. J. Seller, S. L. Biroc, A. Szydlik, J. K. Pinkstaff, F. Tian, S. C. Sinha, B. Felding-Habermann, V. V. Smider and P. G. Schultz, *Proc. Natl. Acad. Sci. U. S. A.*, 2012, **109**, 16101–16106.
23 F. Tian, Y. Lu, A. Manibusan, A. Sellers, H. Tran, Y. Sun, T. Phuong, R. Barnett, B. Hehli, F. Song, M. J. DeGuzman, S. Ensari, J. K. Pinkstaff, L. M. Sullivan, S. L. Biroc, H. Cho, P. G. Schultz, J. DiJoseph, M. Dougher, D. Ma, R. Dushin, M. Leal, L. Tchistiakova, E. Feyfant, H.-P. Gerber and P. Sapra, *Proc. Natl. Acad. Sci. U. S. A.*, 2014, **111**, 1766–1771.
24 E. S. Zimmerman, T. H. Heibeck, A. Gill, X. Li, C. J. Murray, M. R. Madlansacay, C. Tran, N. T. Uter, G. Yin, P. J. Rivers, A. Y. Yam, W. D. Wang, A. R. Steiner, S. U. Bajad, K. Penta, W. Yang, T. J. Hallam, C. D. Thanos and A. K. Sato, *Bioconjugate Chem.*, 2014, **25**, 351–361.
25 M. P. VanBrunt, K. Shanebeck, Z. Caldwell, J. Johnson, P. Thompson, T. Martin, H. Dong, G. Li, H. Xu, F. D'Hooge, L. Masterson, P. Bariola, A. Tiberghien, E. Ezeadi, D. G. Williams, J. A. Hartley, P. W. Howard, K. H. Grabstein, M. A. Bowen and M. Marelli, *Bioconjugate Chem.*, 2015, **26**, 2249–2260.
26 M. W.-L. Popp, J. M. Antos and H. L. Ploegh, *Curr. Protoc. Protein Sci.*, 2009, ch. 15, Unit 15.3.
27 S. Jeger, K. Zimmermann, A. Blanc, J. Grünberg, M. Honer, P. Hunziker, H. Struthers and R. Schibli, *Angew. Chem., Int. Ed.*, 2010, **49**, 9995–9997.
28 P. Strop, S.-H. Liu, M. Dorywalska, K. Delaria, R. G. Dushin, T.-T. Tran, W.-H. Ho, S. Farias, M. G. Casas, Y. Abdiche, D. Zhou, R. Chandrasekaran, C. Samain, C. Loo, A. Rossi, M. Rickert, S. Krimm, T. Wong, S. M. Chin, J. Yu, J. Dilley, J. Chaparro-Riggers, G. F. Filzen, C. J. O'Donnell, F. Wang, J. S. Myers, J. Pons, D. L. Shelton and A. Rajpal, *Chem. Biol.*, 2013, **20**, 161–167.
29 Q. Zhou, J. E. Stefano, C. Manning, J. Kyazike, B. Chen, D. A. Gianolio, A. Park, M. Busch, J. Bird, X. Zheng, H. Simonds-Mannes, J. Kim, R. C. Gregory, R. J. Miller, W. H. Brondyk, P. K. Dhal and C. Q. Pan, *Bioconjugate Chem.*, 2014, **25**, 510–520.
30 R. van Geel, M. A. Wijdeven, R. Heesbeen, J. M. M. Verkade, A. A. Wasiel, S. S. van Berkel and F. L. van Delft, *Bioconjugate Chem.*, 2015, **26**, 2233–2242.
31 P. Dennler, A. Chiotellis, E. Fischer, D. Brégeon, C. Belmant, L. Gauthier, F. Lhospice, F. Romagne and R. Schibli, *Bioconjugate Chem.*, 2014, **25**, 569–578.
32 A. Josten, L. Haalck, F. Spener and M. Meusel, *J. Immunol. Methods*, 2000, **240**, 47–54.
33 J. Buchardt, H. Selvig, P. F. Nielsen and N. L. Johansen, *Biopolymers*, 2010, **94**, 229–235.

34 T. L. Mindt, V. Jungi, S. Wyss, A. Friedli, G. Pla, I. Novak-Hofer, J. Grünberg and R. Schibli, *Bioconjugate Chem.*, 2008, **19**, 271–278.
35 H. Sato, E. Hayashi, N. Yamada, M. Yatagai and Y. Takahara, *Bioconjugate Chem.*, 2001, **12**, 701–710.
36 J. Tominaga, Y. Kemori, Y. Tanaka, T. Maruyama, N. Kamiya and M. Goto, *Chem. Commun.*, 2007, 401–403.
37 G. M. Dubowchik, S. Radia, H. Mastalerz, M. A. Walker, R. A. Firestone, H. Dalton King, S. J. Hofstead, D. Willner, S. J. Lasch and P. A. Trail, *Bioorg. Med. Chem. Lett.*, 2002, **12**, 1529–1532.
38 H. D. King, G. M. Dubowchik, H. Mastalerz, D. Willner, S. J. Hofstead, R. A. Firestone, S. J. Lasch and P. A. Trail, *J. Med. Chem.*, 2002, **45**, 4336–4343.
39 A. Maruani, D. A. Richards and V. Chudasama, *Org. Biomol. Chem.*, 2016, **14**, 6165–6178.
40 M. R. Levengood, X. Zhang, J. H. Hunter, K. K. Emmerton, J. B. Miyamoto, T. S. Lewis and P. D. Senter, *Angew. Chem., Int. Ed.*, 2017, **56**, 733–737.
41 G. M. Dubowchik, R. A. Firestone, L. Padilla, D. Willner, S. J. Hofstead, K. Mosure, J. O. Knipe, S. J. Lasch and P. A. Trail, *Bioconjugate Chem.*, 2002, **13**, 855–869.
42 N. J. Agard, J. A. Prescher and C. R. Bertozzi, *J. Am. Chem. Soc.*, 2004, **126**, 15046–15047.
43 Y. T. Adem, K. A. Schwarz, E. Duenas, T. W. Patapoff, W. J. Galush and O. Esue, *Bioconjugate Chem.*, 2014, **25**, 656–664.
44 R. P. Lyon, T. D. Bovee, S. O. Doronina, P. J. Burke, J. H. Hunter, H. D. Neff-LaFord, M. Jonas, M. E. Anderson, J. R. Setter and P. D. Senter, *Nat. Biotechnol.*, 2015, **33**, 733–735.
45 Y. Shi, X. Fan, W. Meng, H. Deng, N. Zhang and Z. An, *Breast Cancer Res.*, 2014, **16**, R33.
46 P. Dennler, L. K. Bailey, P. R. Spycher, R. Schibli and E. Fischer, *ChemBioChem*, 2015, **16**, 861–867.
47 F. Lhospice, D. Brégeon, C. Belmant, P. Dennler, A. Chiotellis, E. Fischer, L. Gauthier, A. Boëdec, H. Rispaud, S. Savard-Chambard, A. Represa, N. Schneider, C. Paturel, M. Sapet, C. Delcambre, S. Ingoure, N. Viaud, C. Bonnafous, R. Schibli and F. Romagné, *Mol. Pharmaceutics*, 2015, **12**, 1863–1871.
48 S. Chooniedass, R. Dillon, A. Premsukh, P. Hudson, G. Adams, G. MacDonald and J. Cizeau, *Molecules*, 2016, **21**, 1741–1717.

